

Fundamental properties of cooperative contagion processes

Li Chen*

*Robert Koch-Institute, Nordufer 20, 13353 Berlin, Germany
Max Planck Institute for the Physics of Complex Systems, 01187 Dresden, Germany and
School of Physics and Information Technology, Shaanxi Normal University, Xi'an 710062, China*

Fakhteh Ghanbarnejad†

*Robert Koch-Institute, Nordufer 20, 13353 Berlin, Germany and
Max Planck Institute for the Physics of Complex Systems, 01187 Dresden, Germany*

Dirk Brockmann‡

*Robert Koch-Institute, Nordufer 20, 13353 Berlin, Germany and
Institute for Theoretical Biology & Integrative Research Institute for the Life Sciences,
Humboldt Universität zu Berlin, Philippstr. 13, Haus 4, 10115 Berlin, Germany*

We investigate the effects of cooperativity between contagion processes that spread and persist in a host population. We propose and analyze a dynamical model in which individuals that are affected by one transmissible agent A exhibit a higher than baseline propensity of being affected by a second agent B and vice versa. The model is a natural extension of the traditional SIS (Susceptible-Infected-Susceptible) model used for modeling single contagion processes. We show that cooperativity changes the dynamics of the system considerably when cooperativity is strong. The system exhibits discontinuous phase transitions not observed in single agent contagion, multistability, a separation of the traditional epidemic threshold into different thresholds for inception and extinction as well as hysteresis. These properties are robust and are corroborated by stochastic simulations on lattices and generic network topologies. Finally, we investigate wave propagation and transients in a spatially extended version of the model and show that especially for intermediate values of baseline reproduction ratios the system is characterized by various types of wave-front speeds. The system can exhibit spatially heterogeneous stationary states for some parameters and negative front speeds (receding wave fronts). The two agent model can be employed as a starting point for more complex contagion processes, involving several interacting agents, a model framework particularly suitable for modeling the spread and dynamics of microbiological ecosystems in host populations.

PACS numbers: 05.90.+m, 89.75.Hc, 87.23.Cc

I. INTRODUCTION

Contagion processes abound in nature, ranging from the spread of infectious diseases in host populations [1], the spread of information in social networks [2], the adaptation of technology and norms [3, 4], to activation patterns in neural tissue [5, 6], and escape mechanisms from predators in schooling fish [7]. Dynamical computational models are an essential tool for understanding phenomena in all of these contexts. Their application to the spread of infectious diseases has flourished in recent years [8–11], primarily because of the relevance to human health and the spread of human infectious diseases. Dynamical models cover a broad scope in terms of complexity, ranging from qualitative models that focus on universal features of the observed phenomenon [12, 13], network models that account for population structure or host mobility patterns [14–20], to sophis-

ticated, large-scale agent-based models [21, 22] that incorporate high resolution data on multi-scale transportation, demographics, epidemiological factors, and behavioral response rules. State-of-the-art computational models have become remarkably successful in reproducing observed patterns and predicting the trend of ongoing epidemics.

Most epidemic models focus on the transmission dynamics of single, symptomatic pathogenic bacteria or viruses because in most applications it can reasonably be assumed that the phenomena are dominated by host pathogen interactions. A variety of infectious diseases exist, however, that interact either directly or indirectly e.g. by altering the susceptibility of the host with respect to infection with another pathogen. Furthermore, transmissions of bacterial microorganism between host individuals is not restricted to species that cause disease. The transmission and spread of commensal or mutualistic bacteria as part of the host's microbiome is generic, in fact also often required to sustain a healthy, host specific microbiome. Especially the transmission of bacterial species of the human microbiome has attracted much attention in very recent studies [23, 24]. Microbiotic species are part of a complex microbiological ecosystem of a host, with a

* chenl@snnu.edu.cn

† fakhteh@pks.mpg.de

‡ dirk.brockmann@hu-berlin.de

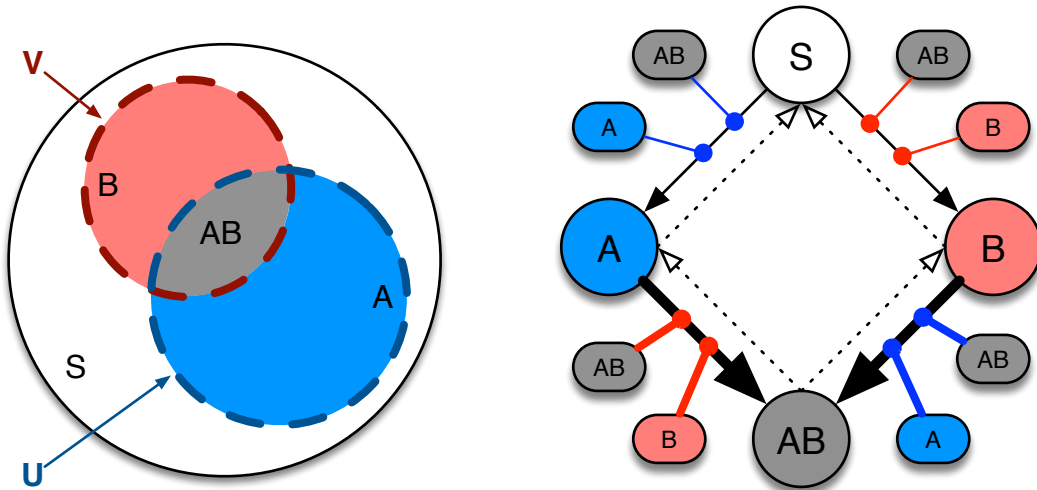


FIG. 1. **Cooperativity of two contagion processes.** Two agents, A and B , spread in a host population. We classify the state of a host individual by letters S (white), A (blue), B (red), and AB (grey) corresponding to being susceptible, infected only by A , infected only by B , and infected by both A and B , respectively. The state of the population can be defined by the subsets \mathcal{S} , \mathcal{A}^+ , \mathcal{B}^+ , $\mathcal{A}^+ \cap \mathcal{B}^+$ corresponding to the sets of susceptibles, infected by A (interior of blue dashed circle), infected by B (interior of red dashed circle), and infected by both (grey area), respectively. Note that the sets \mathcal{A}^+ and \mathcal{B}^+ include individuals in state AB . The relative size (fraction of individuals) of \mathcal{A}^+ , \mathcal{B}^+ , $\mathcal{A}^+ \cap \mathcal{B}^+$ and \mathcal{S} is denoted by u , v , w , and $1 - u - v + w$, respectively. Contagion dynamics is determined by 12 reactions depicted on the right. Susceptibles S acquire A by interacting with individuals from set \mathcal{A}^+ (A or AB individuals) at rate α_A . Likewise, susceptibles S acquire B by interacting with individuals in set \mathcal{B}^+ (B or AB individuals) at rate α_B . Cooperativity means that individuals in state A (B) acquire agent B (A) at higher rates interacting with individuals in set \mathcal{B}^+ (\mathcal{A}^+) symbolized by the thicker interaction lines in the reaction scheme. Dashed lines symbolize recovery events.

densely connected set of metabolic connections [25]. It is reasonable to assume that these interactions, and the presence of particular species in a host's microbiome impacts the propensity of colonization with another. In social science, the adoption of a certain behavioral patterns may impact the propensity to adopt another pattern if exposed to it. Therefore, it is important to understand the basic mechanisms and effects that are generated by interactions of contagion processes in general.

Early network theoretic work focused on competitive coinfection [26–33] with important applications to infection dynamics of virus strains that induce cross immunity. Multiplex network approaches have also been applied in this context [34, 35], in which each contagion process evolves along a different set of links in the same population [26–28, 36].

Only recently, cooperative contagion in which infection with one transmissible agent facilitates infection with another was investigated [37–41]. These studies mainly focused on transient dynamics of the generic SIR (Susceptible-Infected-Recovery) model in which individuals acquire immunity after infection. In Ref. [38], a simple SIR coinfection model was investigated within the framework of cooperative bond percolation. This model exhibits avalanche-like outbreak scenarios, depending on the level of cooperation and the structure of the under-

lying transmission network. Analytical insights were obtained for cooperative bond percolation in multiplex systems [42, 43]. Furthermore, it has been found that highly clustered structures in population aid the proliferation of coinfections, contrary to the effect observed in single disease dynamics [40]. Because most of these models focus on transient SIR dynamics they can't capture situations in which a steady supply of susceptibles permits the existence of a stable endemic state, such as the SIS or SIRS or SIR model with vital processes. Particularly in these systems, some fundamental issues remain elusive: What basic dynamical features can we expect in cooperative contagion processes? To what extent does cooperativity change the classic outbreak scenario, what is the nature of transitions to endemic states? Can we expect multi-stability and multiple thresholds? How does cooperativity impact spatial propagation?

Here we introduce and investigate a model for the dynamics of two transmissible, interacting agents (labeled A and B). The model is based on the well-known SIS model in which host individuals are either susceptible (S) or infected (I). Susceptibles can be infected with either agent. When infected with say A they can transmit A to other susceptibles. Infecteds remain in the infectious state for a typical period after which they recover and susceptible again. The transmission dynamics of agents

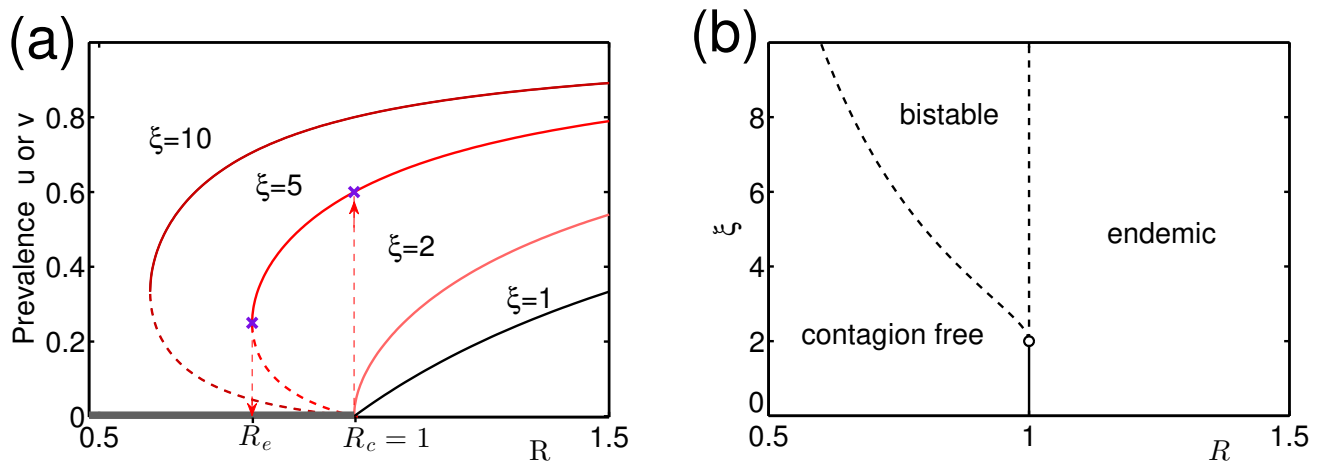


FIG. 2. **Bifurcation analysis of cooperative contagion processes.** (a) For various values of the cooperativity coefficient ξ the stationary states of the symmetric system (Eqs. (6)) are depicted. When ξ is greater than the critical cooperativity $\xi_c = 2$ a regime $R_e < R < R_c$ exists in which the system exhibits three stationary states, the stable trivial state $u = v = 0$ (grey line), another stable endemic state (upper branch, solid red lines) and an unstable intermediate state (dashed red line), see Eqs. (7). In this regime small perturbation to the $u, v = 0$ state will not cause a transition to the endemic branch. Only if perturbations are sufficiently large (crossing the unstable fixed point branch) the system will approach the endemic state. This behavior implies that when subjected to sporadic small perturbations while increasing R , the system will remain near the stable contagion free state until the upper critical point $R_c = 1$ is crossed at which point the system will generate a discontinuous jump, similar to a first order phase transition. The vertical dashed lines illustrate the hysteresis loop. (b) Phase diagram of the system in parameter space, separating three asymptotic states: contagion free, endemic, and bistable, with discontinuous (dashed line) and continuous (solid line) transitions at the interfaces. The circle denotes the tri-critical point at $(R_c = 1, \xi_c = 2)$, which separates the continuous and discontinuous outbreak transitions.

A and B are governed by agent specific baseline reproduction numbers R_A and R_B , respectively that describe the dynamics of an agent in the absence of the other. We incorporate cooperativity by two additional parameters, the cooperativity coefficients ξ_A and ξ_B that capture influence of an infection with A on the subsequent infection with B and vice versa.

Based on this model, we show that cooperativity between contagion processes generates a variety of interesting properties that are absent in single agent dynamics. For sufficiently strong cooperativity, increasing the baseline reproduction number of one or both agents yields abrupt, discontinuous outbreak transitions and multistability (i.e. the coexistence of different stable asymptotic states). Furthermore, cooperativity exhibits dynamical hysteresis, a consequence of the split of the ordinary epidemic threshold into two separate thresholds (an inception and extinction threshold). We derive these features analytically in a deterministic well-mixed model. Their robustness is corroborated by numerical simulations of analogous stochastic dynamical processes on both lattices and generic network systems. Finally we investigate cooperative contagion in spatially extended systems. We show that the interplay of different thresholds and hysteresis yields a rich set of wavefront dynamics and invasion dynamics, e.g. accelerated propagation in certain parameter regimes, stable heterogeneous patterns as well

as negative wavefront speeds (receding wavefronts).

II. COOPERATIVE CONTAGION

Our model is an extension of the generic SIS compartmental model: host individuals are either susceptible (S) or infected (I) and change state by two reactions, the transmission of the infection $S + I \rightarrow 2I$ and recovery $I \rightarrow S$ at rates α and β , respectively. In a well mixed, large, and conserved population the fraction of infected individuals $u(t)$ can be described by $\dot{u} = \alpha u(1 - u) - \beta u$. The basic reproduction ratio is defined by $R = \alpha/\beta$. For $R < 1$ the trivial state $u = 0$ is globally stable. If R is increased beyond the critical threshold $R_c = 1$ the system exhibits a transcritical bifurcation, $u = 0$ becomes unstable and $u = 1 - R^{-1}$ is the stable endemic state in which transmission and recovery events balance. The SIS system thus exhibits a continuous transition as R crosses the critical threshold $R_c = 1$. Analogous stochastic lattice models in which lattice sites can transmit to neighboring sites and recover exhibit the same type of threshold behavior and a continuous phase transition. Here, we consider a generalization of the SIS model that captures the dynamics of two interacting transmissible agents: A and B . A host can be in one of four states S , A , B , and AB , corresponding to susceptible, infected with A but not B , infected with B but not A , and infected with

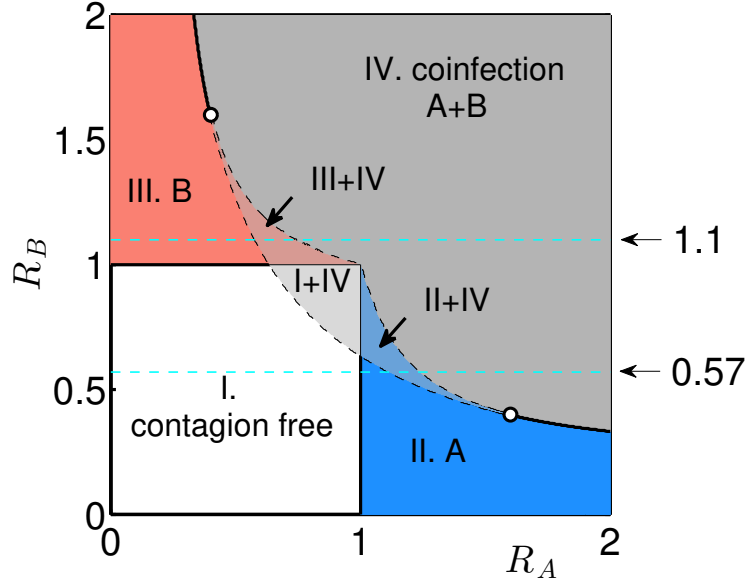
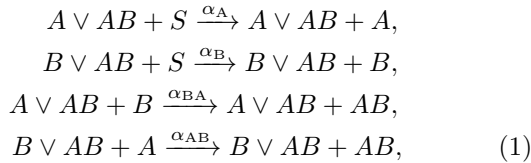


FIG. 3. **Phase diagram of generic cooperative contagion for fixed cooperativity coefficient $\xi = 5$.** In the parameter space spanned by the baseline reproduction ratio R_A and R_B we observe four phases in which only a single stable state exists: S (region I), A (region II), B (region III), and AB (region IV). When baseline reproduction is near unity the system exhibits additional regimes characterized by coexisting stable states (bounded by the black dashed lines): coexistence of S and AB (region I+IV), of A and AB (region II+IV), B and AB (region III+IV). Regimes are separated by different types of bifurcations. Solid lines represents the ordinary transcritical bifurcation, dashed lines represent discontinuous transitions. The black circles denote tri-critical points where bifurcation types merge. The two horizontal dashed lines correspond to the panels depicted in Fig. 4.

both A and B , respectively, see Fig. 1. Transmissions in this system occur by interactions of host individuals in these four different states and can be summarized as follows



where e.g. $A \vee AB$ represents an individual that is either in state A or in state AB such that e.g. the first reaction represents the transmission of agent A to a susceptible individual. The system is defined by four different transmission rates α_A , α_B , α_{BA} , and α_{AB} that correspond to transmission of A to a susceptible, of B to a susceptible, of A to an individual carrying B , of B to an individual carrying A , respectively. For simplicity we assume uniform recovery rates:



Because we focus on cooperative contagion we restrict the transmission rates:

$$\alpha_{BA} = \xi_B \alpha_A \geq \alpha_A, \quad \alpha_{AB} = \xi_A \alpha_B \geq \alpha_B, \quad (3)$$

cooperativity thus implies that $\xi_A, \xi_B \geq 1$. For example, a value $\xi_A = 5$ means that transmission of B to an individual already carrying A is 5-fold the transmission compared to the baseline transmission to an S individual. Based on the above reactions one can obtain a set of ordinary differential equations for the fraction of individuals in each state. The reactions above, however, suggest a more suitable set of compartments \mathcal{S} , \mathcal{A}^+ , \mathcal{B}^+ and $\mathcal{AB} = \mathcal{A}^+ \cap \mathcal{B}^+$ with the corresponding dynamical variables s , u , v , and w : the fractions of susceptibles, individuals infected with A (including those that are also infected with B), individuals infected with B (including those that are infected with A), and individuals infected with both A and B , respectively, see Fig. 1. In the limit of a large, well-mixed host population the dynamics is described by

$$\begin{aligned}
 \dot{u} &= R_A s u + \xi_B R_A (v - w) u - u \\
 \dot{v} &= R_B s v + \xi_A R_B (u - w) v - v \\
 \dot{w} &= \xi_A R_B (u - w) v + \xi_B R_A (v - w) u - 2w, \\
 s &= 1 - u - v + w,
 \end{aligned} \quad (4)$$

where $R_A = \alpha_A/\beta$, $R_B = \alpha_B/\beta$ and time is measured in units of β^{-1} . For cooperativity coefficients $\xi_A = \xi_B = 1$ the above system describes two independent contagion processes: If $R_A, R_B > 1$ the stable en-

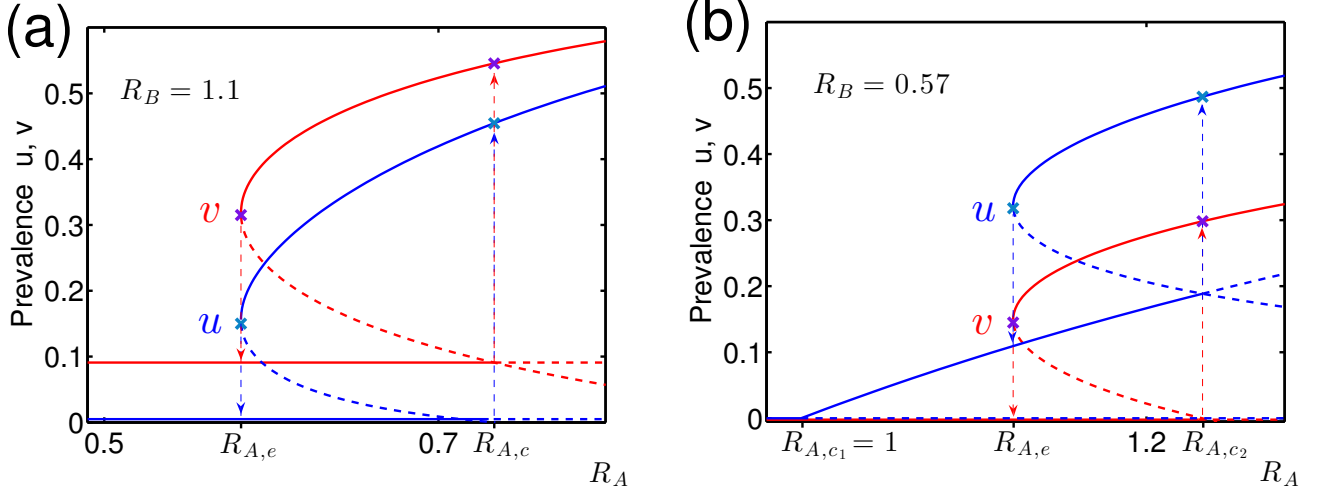


FIG. 4. **Bifurcations in asymmetric cooperative contagion.** The asymptotic prevalence u^* and v^* of agent A and B , respectively, as a function of baseline reproduction ratio R_A for fixed R_B and cooperativity coefficient $\xi = 5$, as indicated in Fig. 3. (a) For $R_B = 1.1$, a hysteresis structure emerges for agent A between $u^* = 0$ and the AB state branch, while for infection B the hysteresis structure spans endemic state ($v^* = 1 - 1/R_B$) and the coinfection AB branch. (b) For subcritical baseline $R_B = 0.57$, prevalence of A exhibits two outbreak transitions: i.) the classical transcritical bifurcation at $R_{A,c1} = 1$, ii.) a saddle node bifurcation with a hysteresis formed between an endemic ($u^* = 1 - 1/R_{A,c1}$) and the coinfecting branch within $R_{A,e} < R < R_{A,c2}$. Note that the second, discontinuous jump in u when R_A is increased beyond $R_{A,c2}$ is caused because the state $v^* = 0$ loses stability at this point.

demographic state is given by $u^* = 1 - R_A^{-1}$, $v^* = 1 - R_B^{-1}$, $w^* = (1 - R_A^{-1})(1 - R_B^{-1})$, and $s^* = (R_A R_B)^{-1}$.

We now consider the effect of cooperativity. In the following and in analogy to the labels used to identify the state of an individual in the population, it is useful to assign the same labels S , A , B , and AB to the potential asymptotic states of the entire host population. We say, e.g., that the system is in state A if only agent A is present in the population, the contagion free state is S , etc.. We begin with a symmetric system in which $\xi_A = \xi_B = \xi$ and identical baseline reproduction ratios $R_A = R_B = R$. In this case the above system reduces to:

$$\begin{aligned} \dot{u} &= Rsu + \xi R(v - w)u - u \\ \dot{v} &= Rsv + \xi R(u - w)v - v \\ \dot{w} &= \xi R[2uw - (u + v)w] - 2w. \end{aligned} \quad (6)$$

Fig. 2 illustrates the bifurcation analysis of the system. When $1 \leq \xi < 2$ the system exhibits a behavior similar to independent contagion processes: At $R = 1$ we observe a transcritical bifurcation yielding a stable endemic population state AB for $R > 1$. This means that even when cooperativity amplifies transmission rates by up to a factor of 2, we see no qualitative dynamical difference.

However, when cooperativity exceeds a critical magnitude, i.e. for $\xi > \xi_c = 2$, a different bifurcation behavior emerges. As R is increased and before the conventional critical point $R_c = 1$ is reached, a saddle-node bifurcation emerges at $R_e = 2\sqrt{\xi - 1}/\xi < 1$. When $R_e < R < R_c$, in addition to the trivial stable state S , two AB stationary

states exist

$$\begin{aligned} u_{\pm}^* &= v_{\pm}^* = \frac{\xi R - 2 \pm \sqrt{\xi^2 R^2 - 4\xi + 4}}{2\xi R}, \\ w_{\pm}^* &= \frac{Ru_{\pm}^*(\xi - 2) + R - 1}{(\xi - 1)R}, \end{aligned} \quad (7)$$

one of which $(u_{\pm}^*, v_{\pm}^*, w_{\pm}^*)$ is stable, the other unstable. Thus, when $R_e < R < R_c$ sufficiently small perturbations to the S state will have no effect as S is stable. However, when perturbations are sufficiently large, the system will approach the endemic AB state with $u_{\pm}^* = v_{\pm}^*, w_{\pm}^*$. Furthermore, when R is increased beyond the critical value $R_c = 1$, state S loses stability and any arbitrarily small perturbation will yield a discontinuous jump to the endemic state, reminiscent of a first order phase-transition. For example when $R = R_c + \varepsilon$ with $0 < \varepsilon \ll 1$ the stable endemic state is $u_{\pm}^* = v_{\pm}^* \approx (\xi - 2)/\xi$, $w_{\pm}^* \approx (\xi - 2)^2/\xi(\xi - 1)$. So if say $\xi = 10$ this yields an endemic state in which 71% of the population is in state AB , immediately after R_c is crossed. Cooperative contagion also exhibits hysteresis: Starting with $R > R_c$ and state AB , decreasing R across the critical value R_c from above will not result in immediate extinction. A high endemic state is maintained until the eradication threshold R_e is reached, which can be substantially smaller than the ordinary epidemic threshold R_c . Decreasing R below R_e will then yield a sudden collapse of AB into S .

Eqs. (6) capture the symmetric special case of the more general system defined by Eqs. (4), the latter of which has four parameters, R_A , R_B , ξ_A , and ξ_B . Fig. 3 illustrates the phase diagram for a more general choice of

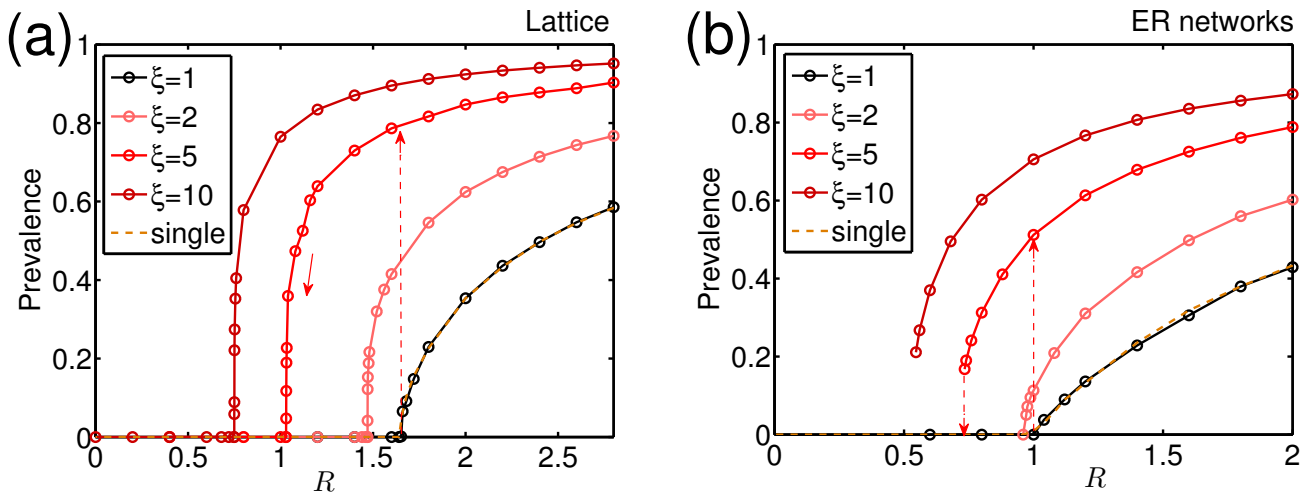


FIG. 5. **Phase transitions of prevalence (either A or B) in stochastic network models.** Cooperative contagion on (a) two dimensional square lattices (with size 100×100) and (b) ER networks (with network size $N = 10000$ and average degree $\langle k \rangle = 4$). The reproduction ratio is defined as $R = \langle k \rangle \alpha / \beta$ where α is the transmission rate across a link. To investigate the extinction threshold, the simulations (with Gillespie algorithm) are initiated with complete prevalence. The transitions is obtained by decreasing R . Outbreak transitions are only possible when R is close to the threshold of single infection if the population starts with tiny infected nodes, e.g. two remote infected nodes with A, B respectively. The thresholds of single infection R_c are around 1.64 and 1 respectively in (a) and (b), while a smaller eradication threshold is expected in strong cooperative cases as shown, therefore a hysteresis structure is formed in line with the above mean field theory.

these parameters. Fixing the cooperativity coefficients to $\xi_A = \xi_B = 5$ we investigated the phases of the system as a function of baseline reproduction ratios R_A and R_B . Apart from the expected stable states we observe a rich variety of bistable states in the region in which baseline reproduction is near unity, as is illustrated in Fig. 4. For example, when $R_B = 1.1$ and starting with $R_A \approx 0$ the system is initially in state B . Increasing R_A further a saddle-node bifurcation occurs and the system enters a regime in which B and AB are both stable. When $R_B < 1$, e.g. $R_B = 0.57$, increasing R_A first yields an ordinary transcritical bifurcation to the A state, followed by a second bifurcation into a regime in which A and AB are stable, and finally, a third bifurcation into the regime in which only AB is stable, see also Fig. 3. A key property of the system is that the complexity of transitions is only observed for baseline reproduction ratios near unity. If one baseline reproduction is too low or too high, only a single ordinary transitions and no state coexistence is observed. This is an interesting property from an evolutionary point of view. When new strains of transmissible agents emerge, typically they are not adapted to the host and possess baseline reproduction not significantly larger than unity, or even smaller. Cooperativity with other transmissible agents and coexistence of stable endemic states may present an opportunity for developing a species rich system with higher evolvability. This type of complexity is expected to increase dramatically when more than two transmissible agents are involved, yielding a potentially rich space of stable states and an increasing complexity in phase separation manifolds in

parameter space.

The deterministic model discussed above cannot account for fluctuations or population heterogeneities. An important question is therefore whether the observed phenomena prevail in a more complex scenario in which transmissions and recovery events are stochastic, the host population is finite and not every host interacts with every other host at equal rates. Typically, stochastic effects in a well-mixed system are modeled by birth-death type stochastic processes equivalent to the reactions depicted in Fig. 1 and generating solutions to the corresponding master-equation for a fixed but finite population size N . Population heterogeneities are typically addressed by modeling these processes on fixed network topologies or lattices in which host individuals only interact with the neighbors defined by the network links. In order to address the robustness of effects and properties derived for the deterministic system of Eqs. (4) we investigated cooperative contagion dynamics in a stochastic 2d-lattice system and Erdős-Rényi (ER) network with equal mean degree and number of nodes. The results are compiled in Fig. 5. In both cases, we observe hysteresis, and a separation of extinction and outbreak thresholds for large cooperativity coefficients ξ . Interestingly, the extinction transition is continuous in the lattice, a consequence of the local coupling of the system. The ER network exhibits discontinuous transitions, as predicted by the above mean field treatment. This is not surprising as the ER network is topologically more similar to the well-mixed scenario. Based on these observations, we believe that the key features of cooperative contagion can

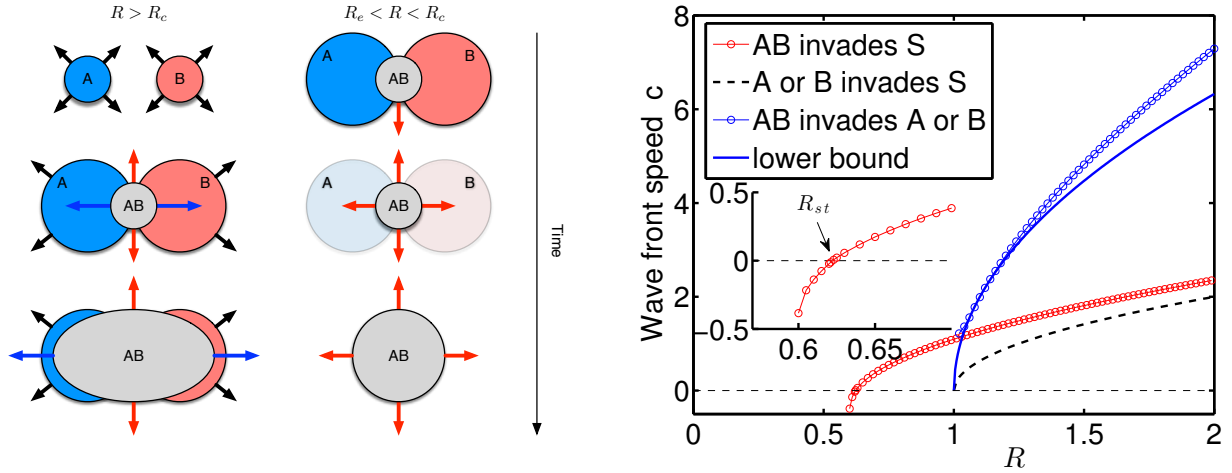


FIG. 6. **Spatial dynamics of cooperative contagion processes.** Left: When $R > R_c$ initially separated region of only A or B affected regions grow with a front speed equivalent to single SIS dynamics, $c_0 \propto \sqrt{(R-1)D}$ (black arrows). When the wave fronts touch, a region of coinfection emerges (grey). This region touches the regions of susceptible (white background) and on each side region that are dominated by either A or B yielding two new front speeds associated with AB invading A or B (blue arrow) and AB invading S (red arrow). Invasion of AB into the susceptible region occurs at a speed $c_{AB \rightarrow S} > c_0$ the blue/red regions occurs at a speed $c_{AB \rightarrow A/B} > c_{AB \rightarrow S}$. In this transient phase, the patterns is shaped by three front speeds of different magnitude. This implies that the intermittent AB invasion will take over the entire pattern and eventually only the AB region will propagate into the susceptible region. When $R < R_c$ initially separated A and B regions cannot be sustained and will relax to the contagion free state. However, if initially a small overlap exists (a nucleation of AB) the pattern will eventually converge to AB invading S as well despite the fact that $R < R_c$. Right: Comparison of the three wave front speeds ($c_{AB \rightarrow S}$ red circled line, $c_{A/B \rightarrow S} = c_0$ black dashed, $c_{AB \rightarrow A/B}$ blue circled line) as a function of R in 1d space, together with a lower analytic bound for $c_{AB \rightarrow A/B} \approx \sqrt{\xi(R-1)D} = \sqrt{\xi}c_0$ (blue solid line). The inset shows that in the invasion of AB into the susceptible region, the speed $c_{AB \rightarrow S}$ is positive for $R > R_{st}$, and negative for $R_e < R < R_{st}$, with $R_{st} = 0.62218(4)$ and $R_e = 0.6$. Parameters: $\xi = 10$, $D = 1$.

be expected also in more realistic, structured populations [44].

III. WAVE PROPAGATION IN SPATIALLY EXTENDED SYSTEMS

An important aspect of contagion processes is their spatial propagation. When simple contagion processes with $R > 1$ are seeded in a spatially homogeneous susceptible host population and contagion dynamics is combined with diffusive dispersal of the host these systems typically exhibit propagating wavefronts that travel at constant speeds. The endemic state invades the unstable S domain. The generic SIS contagion process, e.g., can be described by

$$\partial_t u = R(1-u)u - u + D\partial_x^2 u, \quad (8)$$

where $u = u(\mathbf{x}, t)$ is the density of infected individuals at location \mathbf{x} at time t . The combination of local initial exponential growth (for $R > 1$) and diffusion yields a front-speed depending on the basic reproduction ratio and diffusion coefficient D : $c = 2\sqrt{(R-1)D}$. This is a generic feature of processes that exhibit pulled fronts [45]. Given the more complex nature of cooperative coinfection, especially the dynamical bistability for intermediate baseline

reproduction ratio $R_e < R < R_c$ and large cooperativity coefficient ξ , we can expect a richer set of phenomena when cooperative contagion processes expand in space. To account for a diffusing host we extend Eqs. (4) and consider the corresponding reaction-diffusion system:

$$\begin{aligned} \partial_t u &= f_u(u, v, w) + D\partial_x^2 u \\ \partial_t v &= f_v(u, v, w) + D\partial_x^2 v \\ \partial_t w &= f_w(u, v, w) + D\partial_x^2 w \end{aligned} \quad (9)$$

where D in last terms is the diffusion coefficient and the functions f_u , f_v , and f_w are the same as on the rhs. of Eqs. (6). The dynamical variables are function of time t and space \mathbf{x} , e.g. $u = u(\mathbf{x}, t)$. We assume that the diffusion coefficient is constant and independent of the state of a host individual primarily focusing on contagion processes that do not affect the host's dispersal behavior. We also consider a constant overall density which implies that $s = 1 - u - v + w$ at every position \mathbf{x} . As before we use labels S , A , B and AB to refer to region that are contagion free, only affected by A , only affected by B , and both A and B , respectively.

The system defined by Eqs. (9) exhibits a range of front velocities, each one corresponding to different states invading regions in a different state. For example a localized A -patch invades an S -region at a different speed

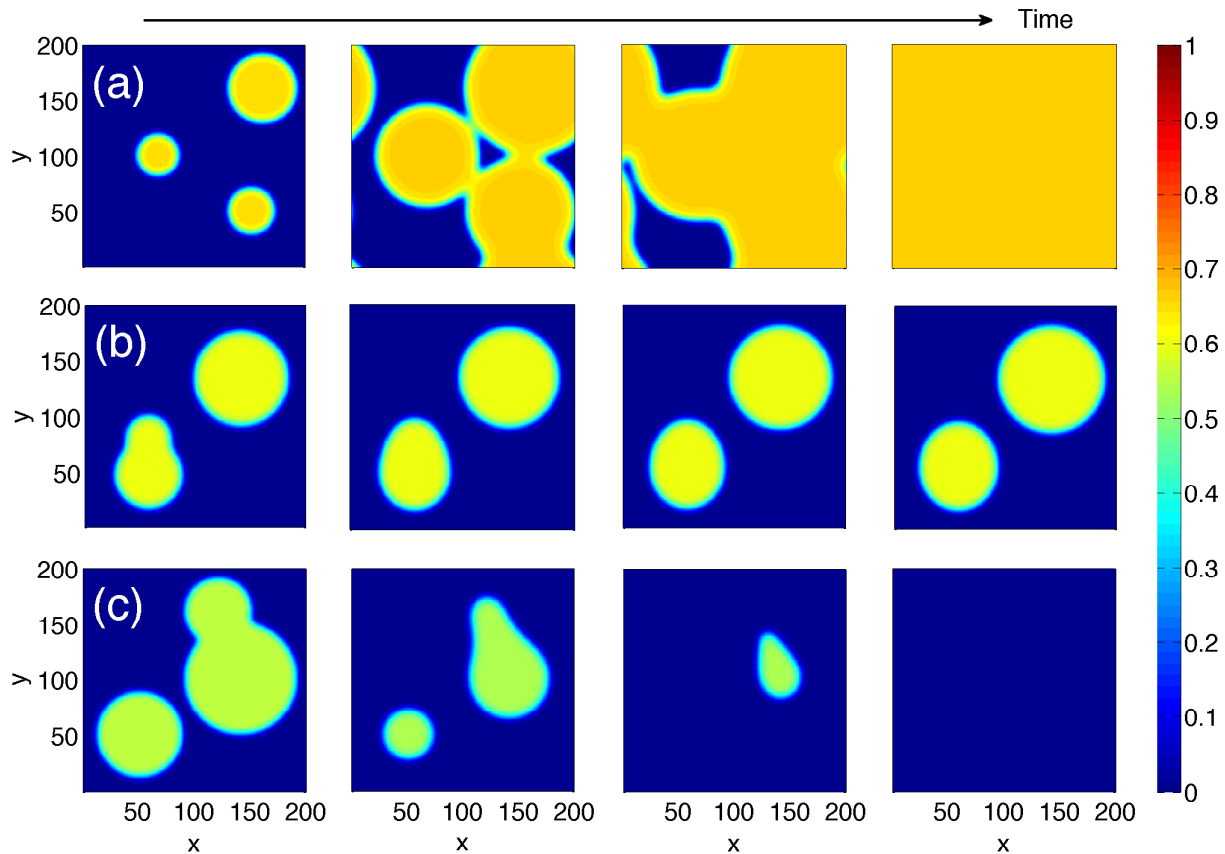


FIG. 7. **Three typical contagion propagation modes in 2d space.** Top panels (a): forward propagation ($R = 0.65$). Middle panels (b): standing front ($R = R_{st} = 0.62671(4)$). Bottom panels (c): backward propagation ($R = 0.61$). The infected fraction $1 - s$ is color coded. The sequence (from left to right) of panels depicts the time course of the infected regions at time $t=0, 100, 200, 300$, respectively. Here R_{st} is slightly different from the value in 1d space, up to the dimension correction. Initial conditions start from some randomly infected round regions with random radius as shown in the first column. Other parameters: $D = 1$, $\xi = 10$, where $R_e = 0.6$.

than a uniform B -region (turning the latter into an AB -region). A localized AB -patch invades an S -region differently than an A -region. To understand the asymptotics and transients of the system we first consider a uniform population in state S , with the exception of two localized patches, each being in state A and B respectively and separated by some distance, see Fig. 6. When $R > R_c$ cooperative contagion plays no role at the beginning, each patch will expand at a constant front speed of $c_0 \propto \sqrt{(R-1)D}$. Once these growing patches touch, cooperativity kicks in at the A - B interface. The emerging AB -nucleus has interfaces to the A and B regions as well as to the S region. For $\xi > 1$ the invasion of AB into the S -region is faster at a speed $c_{AB \rightarrow S} > c_0$ as expected. Interestingly, the invasion of the AB -region into A -region (and B -region) occurs at an even higher speeds $c_{AB \rightarrow A, B} > c_{AB \rightarrow S}$. Using a propagating wave ansatz $u = u(x-ct)$ for a 1-d spatial support (analogously for variables v and w) one can compute a lower bound $c_{AB \rightarrow A, B} \approx \sqrt{\xi(R-1)D} = \sqrt{\xi}c_0$. Because $c_{AB \rightarrow A, B} > c_{AB \rightarrow S}$ the system will eventually converge

to a uniform AB -region that spreads at speed $c_{AB \rightarrow S}$. Regions affected only by one agent will not persist. This effect of enhanced wave-front speed might be particularly relevant in situations in which a covert, unknown and commensal agent is endemic in some region and a known process with known baseline reproduction ratio expands somewhere else in the system at a speed that is computed based on its baseline reproduction ratio. If this front enters the region in which the unknown but highly cooperative covert agent prevails, a sudden but potentially unexpected boost in the proliferation of the initial spreading process could occur.

In the bistable region $R_e < R < R_c$, isolated islands of A nor B cannot persist. If we initialize the system with A and B patches that share a small overlapping region in the AB state cooperativity can yield the survival of the AB state while the homogeneous A and B states fade. The remaining AB patch then proliferates at speed $c_{AB \rightarrow S}$. Interestingly, we observe negative propagation speed in this regime, $c_{AB \rightarrow S} < 0$, which implies a receding AB -region. This behavior is caused by the

dispersal of A or B affected individuals into the S -region in which the S -state is also stable. Once individuals enter this state, they have a higher likelihood of becoming susceptible than being colonized by both agents. The wavefront acts as a drain for infected agents and a competition exists between the supply of new agents of type A or B and the diffusive dilution of their concentration. For a critical choice of parameters, e.g. the baseline reproduction ratio we observe a stationary heterogeneous solution, an immobile front, that separates S from AB regions. Figure 7 illustrating the three typical propagation modes in 2d space are depicted (see also the movies in the Supplemental Materials [46]).

IV. DISCUSSION

We present a reaction kinetic model for the dynamics of cooperative contagion of the susceptible-infected-susceptible class. The most prominent property of the model is the existence of discontinuous transitions to an endemic state when the traditional outbreak threshold is crossed and a separation of outbreak and extinction thresholds, the magnitude of which depends on the degree of cooperativity. Although we derive the key properties analytically and numerically in a deterministic model suitable for large, well-mixed populations, we observe the key features of discontinuous transitions also in a stochastic network variant of the model. The system of two cooperating agents that proliferate in a host populations exhibits diverse properties when spatial diffusion is incorporated yielding different types of transients and

spreading speeds.

Although we discussed the model predominantly in the context of the spread of transmissible diseases, the model is sufficiently generic to be applied to other transmissible contagion processes that influence each other cooperatively, e.g. the adoption of one technology may increase the infection of a user with another type of technology which may then occur explosively or at different speeds than expected.

Considering a model for only two interacting agents is foundation that can easily be generalized to a larger number, potentially a network, of interacting agents. If the baseline reproduction of a family of transmissible agents is in the critical regime, we expect in such a system a diverse set of stable configurations and we believe that the model presented here is a helpful starting point for investigating these more general systems.

ACKNOWLEDGEMENT

L.C. and F.Gh. would like to thank W. Cai and P. Grassberger for valuable comments and discussions. D.B. acknowledges fruitful discussion with Osamah Hamouda and Imbish Mortimer. L.C. also would like to thank the hospitality of Beijing Computational Science Research Center (CSRC) for a pleasant stay during the final revision stage.

Author contributions: L.C., F.Gh, D.B. conceived research, L.C. and D.B. developed dynamical model, L.C., D.B. theoretical, analytical treatment of mean field and spatial model, L.C. performed numerical analysis. D.B. and L.C. wrote manuscript.

-
- [1] R. M. Anderson and R. M. May, *Infectious diseases of humans: dynamics and control*, (Oxford University Press, Oxford New York, 1992).
 - [2] D. Gruhl, R. Guha, D. Liben-Nowell, and A. Tomkins, *Information diffusion through blogspace*, In Proceedings of the 13th international conference on World Wide Web, pages 491501, ACM (2004).
 - [3] C. Bicchieri, *The grammar of society: The nature and dynamics of social norms*, (Cambridge University Press, 2005).
 - [4] E. M. Rogers. *Diffusion of innovations*, (Simon and Schuster, 2010).
 - [5] G. Buzsáki, *Rhythms of the Brain*, (Oxford University Press, 2006).
 - [6] G. Buzsáki and A. Draguhn, *Neuronal oscillations in cortical networks*, *Science* **304**,1926, (2004).
 - [7] W. E. Cooper Jr and D. T. Blumstein, *Escaping from predators: an integrative view of escape decisions*, (Cambridge University Press, 2015).
 - [8] L. Hufnagel, D. Brockmann, and T. Geisel, *Forecast and control of epidemics in a globalized world*, *Proc. Natl. Acad. Sci. USA* **101**, 15124 (2004).
 - [9] V. Colizza, A. Barrat, and M. Barthelemy *et al.*, *Predictability and Epidemic Pathways in Global Outbreaks of Infectious Diseases: The SARS Case Study*, *BMC Med.* **5**, 34 (2007).
 - [10] C. Fraser, C. A. Donnelly, and S. Cauchemez *et al.*, *Pandemic Potential of a Strain of Influenza A (H1N1): Early Findings*, *Science* **324**, 1557 (2009).
 - [11] D. Brockmann and D. Helbing, *The hidden geometry of complex, network-driven contagion phenomena*, *Science* **342**, 1137 (2013).
 - [12] W. O. Kermack and A. G. McKendrick, *A Contribution to the Mathematical Theory of Epidemics*, *Proc. R. Soc. A* **115**, 700 (1927).
 - [13] H. W. Hethcote, *The mathematics of infectious diseases*, *SIAM Review* **42**, 599 (2000).
 - [14] A. Barrat, M. Barthélemy, and A. Vespignani, *Dynamical Processes on Complex Networks*, (Cambridge, 2008).
 - [15] R. Pastor-Satorras and A. Vespignani, *Epidemic Spreading in Scale-Free Networks*, *Phys. Rev. Lett.* **86**, 3200 (2001).
 - [16] V. Colizza, A. Barrat, M. Barthélemy, and A. Vespignani, *The Role of the Airline Transportation Network in the Prediction and Predictability of Global Epidemics*, *Proc. Natl. Acad. Sci. USA* **103**, 2015 (2006)

- [17] D. Brockmann, L. Hufnagel, and T. Geisel, *The scaling laws of human travel*, Nature **439**, 462 (2006).
- [18] M. C. González, C. A. Hidalgo, and A-L Barabási, *Understanding individual human mobility patterns*, Nature **453**, 779 (2008).
- [19] D. Balcan, V. Colizza, B. Gonçalves, H. Hu, J. J. Ramasco, et al. *Multiscale Mobility Networks and the Spatial Spreading of Infectious Diseases*, Proc. Natl. Acad. Sci. USA **106**, 21484 (2009).
- [20] V. Belik, T. Geisel, and D. Brockmann *Natural Human Mobility patterns and Spatial Spread of Infectious Diseases*, Phys. Rev. X **1**, 011001 (2011).
- [21] S. Eubank, H. Guclu, V. S. A. Kumar, et al. *Modeling Disease Outbreaks in Realistic Urban Social Networks*, Nature **429**, 180 (2004).
- [22] W. V. den Broeck, C. Gioannini, B. Goncalves, et al., *The GLEaMviz Computational Tool, a Publicly available Software to Explore Realistic Epidemic Spreading Scenarios at the Global Scale*, BMC Infect. Dis. **11**, 37 (2011).
- [23] F. Sommer and F. Bäckhed, *The gut microbiota - masters of host development and physiology*, Nature Rev. Microbiol. **11**, 227 (2013).
- [24] K. Z. Coyte, J. Schluter, and K. R. Foster, *The ecology of the microbiome: Networks, competition, and stability*, Science **350**, 663 (2015).
- [25] A. Zelezniak, S. Andrejev, O. Ponomarova, D. R. Mende, P. Bork, and K. R. Patil, *Metabolic dependencies drive species co-occurrence in diverse microbial communities*, Proc. Natl. Acad. Sci. USA **112**, 6449 (2015).
- [26] S. Funk and V. A. A. Jansen, *Interacting epidemics on overlay networks*, Phys. Rev. E **81**, 036118 (2010).
- [27] V. Marceau, P. -A. Noël, L. Hébert-Dufresne, A. Allard A, L. J. Dubé, *Modeling the Dynamical Interaction between Epidemics on Overlay Networks*. Phys. Rev. E **84**, 026105 (2011).
- [28] F. D. Sahneh and C. Scoglio, *Competitive Epidemic Spreading over arbitrary multilayer networks*. Phys. Rev. E **89**, 062817 (2014).
- [29] M. E. J. Newman, *Threshold Effects for Two Pathogens Spreading on a Network*, Phys. Rev. Lett. **95**, 108701 (2005).
- [30] Y. -Y. Ahn, H. Jeong, N. Masuda, and J. D. Noh, *Epidemic Dynamics of Two Species of Interacting Particles on Scale-Free Networks*, Phys. Rev. E **74**, 066113 (2006).
- [31] B. Karrer and M. Newman, *Competing Epidemics on Complex Networks*, Phys. Rev. E **84**, 036106 (2011).
- [32] C. Poletto, S. Meloni, V. Colizza, Y. Moreno, A. Vespignani, *Host Mobility Drives Pathogen Competition in Spatially Structured Populations*, PLOS Computational Biology **9**, e1003169 (2013).
- [33] C. Poletto, S. Meloni, A. Van Metre, V. Colizza, Y. Moreno, and A. Vespignani, *Characterising two-pathogen competition in spatially structured environments*, Sci. Rep. **5**, 7895 (2015).
- [34] S. V. Buldyrev, R. Parshani, G. Paul, H. E. Stanley, and S. Havlin, *Catastrophic cascade of failures in interdependent networks*, Nature, **464**, 1025 (2010).
- [35] M. De Domenico, A. Solé-Ribalta, E. Cozzo, M. Kivela, Y. Moreno, M. A. Porter, S. Gómez, and A. Arenas, *Mathematical Formulation of Multilayer Networks*, Phys. Rev. X **3**, 041022 (2013).
- [36] J. Sanz, C.-Y. Xia, S. Meloni, and Y. Moreno, *Dynamics of Interacting Diseases*, Phys. Rev. X **4**, 041005 (2014).
- [37] L. Chen, F. Ghanbarnejad, W. Cai, and P. Grassberger, *Outbreaks of Coinfections: the Critical Role of Cooperativity*, Europhys. Lett. **104**, 50001 (2013).
- [38] W. Cai, L. Chen, F. Ghanbarnejad, and P. Grassberger, *Avalanche-Outbreaks Emerging in Cooperative Contagions*, Nature Phys. **11**, 936 (2015).
- [39] P. Grassberger, L. Chen, F. Ghanbarnejad, and W. Cai, *Phase Transitions in Cooperative Coinfections: Simulation Results for Networks and Lattices*, Phys. Rev. E **93**, 042316 (2016).
- [40] L. Hébert-Dufresne and B. M. Althouse, *Complex dynamics of synergistic coinfections on realistically clustered networks*, Proc. Natl. Acad. Sci. USA **112**, 10551 (2015).
- [41] H. -K. Jassen and O. Stenull, *First-order phase transitions in outbreaks of co-infectious diseases and the extended general epidemic process*, Europhys. Lett. **113**, 26005 (2016).
- [42] A. Allard, L. Hébert-Dufresne, J.-G. Young, and L. J. Dubé, *General and exact approach to percolation on random graphs*, Phys. Rev. E **92**, 062807 (2015).
- [43] N. Azimi-Tafreshi, *Cooperative epidemics on multiplex networks*, Phys. Rev. E **93**, 042303 (2016).
- [44] An online interactive d_3 webpage is available for playing at <http://rocs.hu-berlin.de/D3/cosis/>.
- [45] J. D. Murray, *Mathematical Biology II: Spatial Models and Biomedical Applications*, (Third Edition, Springer Press, 2003).
- [46] See Supplemental Material in the attached files for movies illustrating the three wave propagation modes.